

ALTERATION, ORE MINERALOGY, AND FLUID INCLUSION MICROTHERMOMETRY OF THE RORAH KADAL QUARTZ VEIN IN CIBALIUNG GOLDFIELD, WESTERN JAVA, INDONESIA

Agus Didit Haryanto^{1,2}, Mega Fatimah Rosana², Thomas Tindell¹, Jillian Aira Sibal Gabo¹, Haris Yusuf³, and Kotaro Yonezu¹

¹ Department of Earth Resources Engineering, Faculty of Engineering, Kyushu University, Fukuoka, Japan, e-mail: agus-didit@mine.kyushu-u.ac.jp

² Department of Geology, Padjadjaran University, Jl. Raya Jatinangor Km 21, Sumedang, Indonesia

³ PT. Cibaliung Sumberdaya, Pandeglang, Banten, Indonesia

Received Date: April 10, 2015

Abstract

The Rorah Kadal vein is located in the Cibaliung goldfield, Western Java, Indonesia. The vein is hosted by the Miocene Honje Igneous Complex and composed of sequences of basalt-andesite lava flows, volcanic breccia, and overlain by tuff. The paper is tending to describe occurrence, alteration, mineralogy, and fluid inclusion microthermometry of the Rorah Kadal gold-bearing quartz vein to understand the process and formation condition of gold mineralization. The Rorah Kadal is a single vein trending NW direction and about 700 meters parallel to main Cibaliung vein. The alteration consists of illite/smectite mixed layer mineral-adularia-quartz, chlorite-chlorite/smectite mixed layer mineral, and illite-illite/smectite mixed layer mineral-calcite-quartz zones. The vein types are colloform-crustiform band, breccia, vug, cockade, and comb, which are mainly composed of quartz and adularia. Based on quartz textures, three stages of mineralization are recognized: Stage-1 colloform-crustiform; Stage-2 hydrothermal breccia; and Stage 3- late stage quartz veinlet textures. The ore mineralogy of the Rorah Kadal quartz vein is mainly pyrite, chalcopyrite, galena, sphalerite, electrum, and aguilarite. Fluid inclusion temperatures from five drill core quartz samples ranges from 180 to 330 °C, with salinities varying from 1.2 to 4.0 wt% NaCl. The Rorah Kadal vein has slightly high fluid temperature and salinity as compared to Cikoneng and Cibitung veins of the Cibaliung goldfield. This data suggests that the hydrothermal fluids appear to have formed from low temperature and low salinity fluids in near neutral pH environment.

Keywords: Cibaliung, Epithermal, Fluid inclusion, Rorah Kadal, Western Java

Introduction

The western Java area of Indonesia is well known as an epithermal gold-silver metallogenic province that hosts the inactive mines of Cikotok and Cikidang and the active Pongkor mine. The metallogenic province is mainly centered in the Bayah Dome [1,2] and limited to the Honje Complex [3-5]. The Rorah Kadal vein is situated in the Cibaliung gold mine tenement. The Cibaliung gold mine is operated by PT Cibaliung Sumberdaya, a subsidiary of PT Antam Tbk. The mine is located about 230 km southwest of Jakarta and approximately 70 km west of the Bayah Dome (Fig. 1). Several gold-bearing quartz veins have been identified, such as Cikoneng, Cibitung, Cibeber, Rorah Kadal, and Cikeni veins. There are two veins currently mined, which are the Cikoneng and Cibitung ore shoots that were discovered in 1992 and 1997, respectively [6]. The resources of Cibaliung was reported at 1.5 Mt at 9.8 g/t Au and 83 g/t Ag [6]. The first pour of gold was in 2010 with

an ore production rate of 220,000 ton per annum. To date, however, there is no study conducted on the other veins, such as the Cibeber, Cikeni, and Rorah Kadal (Figure 2).

In 2011-2012, an intensive drilling program was undertaken to investigate the Rorah Kadal quartz vein. Therefore it is important to add to the mine life of the Cibaliung goldfield. However, no detailed study of this vein has been reported. The aim of this paper is to describe occurrence and mineralogy of the Rorah Kadal gold-bearing quartz vein for understanding of process and condition in gold mineralization in the studied area. All the samples used in this study were obtained from drill holes and outcrops.

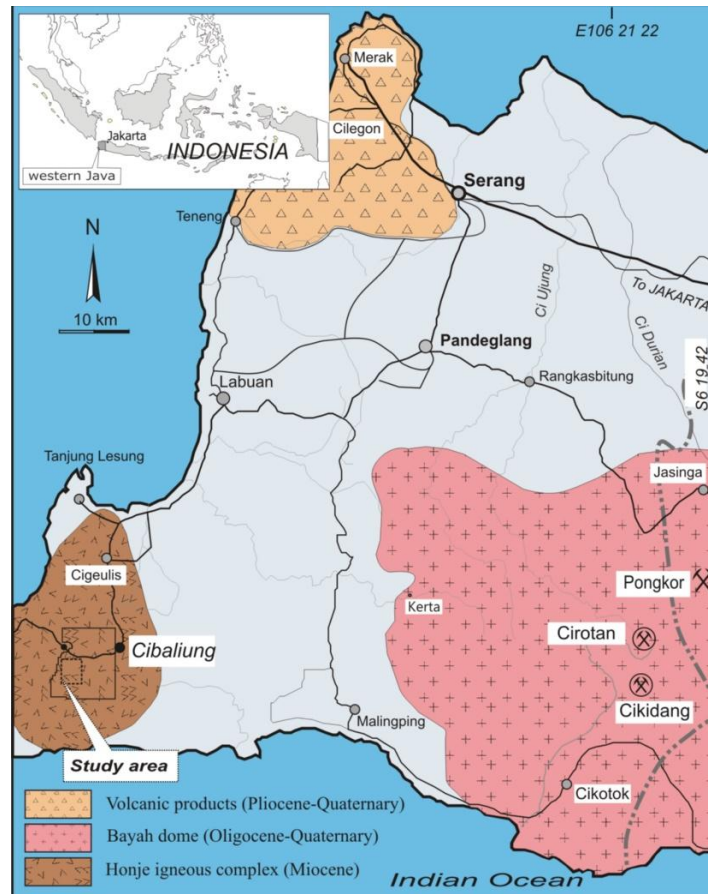


Figure 1. Simplified map of the volcanic complex showing several active and inactive gold mines of the Cibaliung area and western Java (Modified after [1])

Geological Setting

The Cibaliung goldfield is situated in the middle portion of the Sunda-Banda magmatic arc. This Neogene magmatic arc is a transition zone stretching from the northwest-trending right-lateral strike-slip fault that dominates the movement along the Sumatra segment of the arc to the east-west oriented compression faulting in Java Island [7].

Cibaliung area is covered by the Honje Igneous Complex, which is located 15 km west from Bayah Dome, a well-known gold district in western Java [1,2,8]. The Honje Igneous Complex and the Bayah Dome have similar igneous activities, with both complexes characterized by calc-alkaline rhyolitic to andesitic rocks and small intrusive stocks [1].

The Honje Igneous Complex was formed in a back-arc rifting environment equivalent to that of the Bayah Dome. The Honje Igneous Complex is strongly folded and faulted, characterized by a north-trending structural high bordered by west-dipping normal faults

along the Java coast to the west, and east dipping normal faults under the sedimentary depression to the east. The oldest rock unit is the Honje Formation at 11.4 ± 0.8 Ma [4]. The rock units are composed of thick lava flows of basaltic andesite to andesite and volcanic breccia. The Honje Formation is unconformably overlain by massive flat lying sheets of dacitic tuff, referred to as the Cibaliung Tuff with an age of 4.9 ± 0.6 Ma [4,9].

Local Geology

The Cibaliung goldfield is reported as a low sulfidation epithermal type deposit [3-5]. The Cibaliung host rocks are grouped into altered and unaltered rock sequences. The altered host rocks are part of the Honje Formation, whereas the unaltered rocks are related to the Cibaliung Tuff [4]. The Honje Formation is exposed along the Citeluk River valley and in the low-lying areas in the southwestern portion of the Cibaliung mine site. According to [9, 10], the Honje volcanic unit consists of basaltic andesite lava flows and volcanic breccias with sporadic intercalated tuffaceous sediments. The volcanic flows are massive whereas the volcanic breccias are auto-brecciated flows and hyaloclastites. Several sub-volcanic andesite plugs and dikes intrude the Honje Formation in the vicinity of Cibitung. The intrusive rocks are commonly porphyritic-aphanitic with dominant plagioclase and pyroxene phenocrysts.

The Cikoneng and Cibitung quartz veins occur within a NW-trending fault corridor forming a graben or pull-apart basin [3,9]. The Rorah Kadal vein occurs parallel to these two veins within the complex structure, at about 700 meters south of the Cibitung ore shoot (Figure 2).

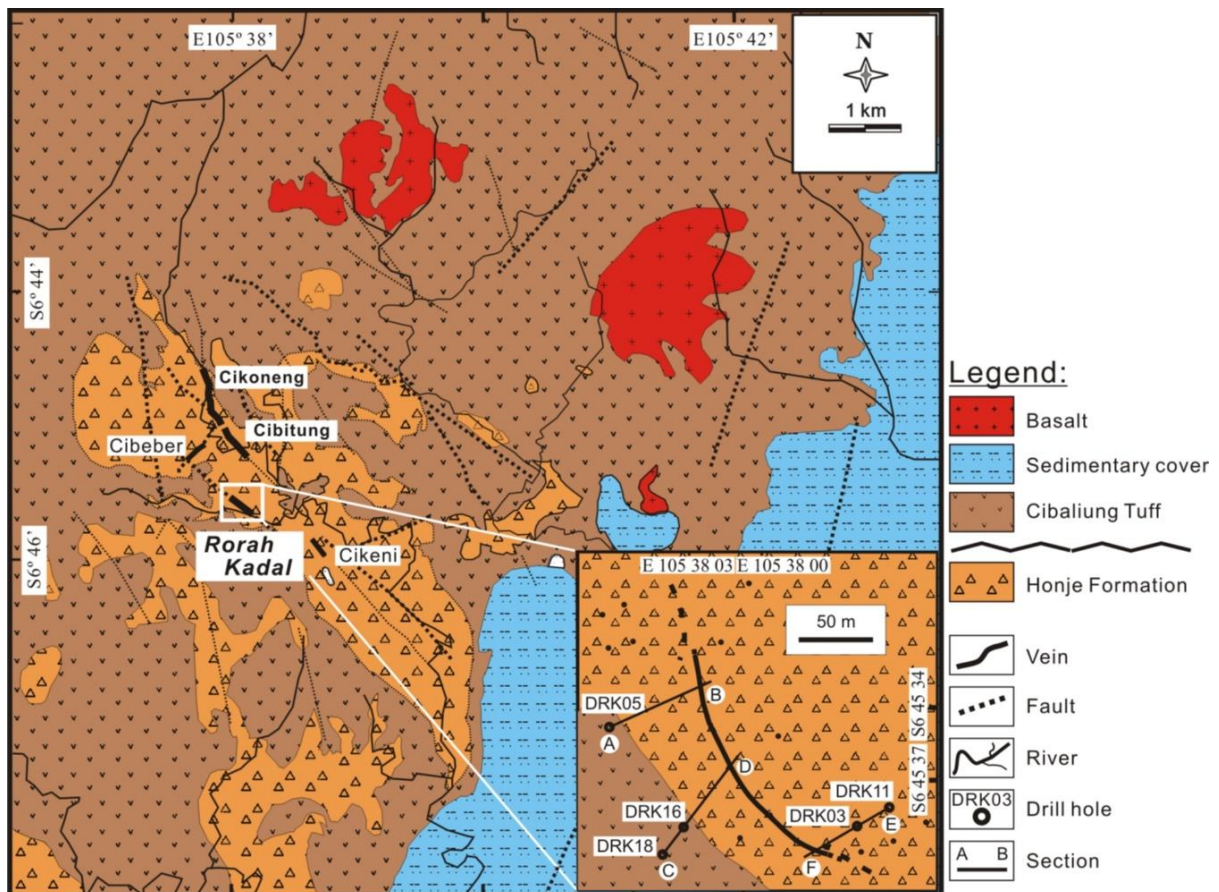


Figure 2. Local geology of study area showing the Rorah Kadal, Cikoneng, and Cibitung veins (modified after [6]). Inset map showing Rorah Kadal vein and drill hole location

Analytical Methods

The data used in this study was obtained from five diamond drill holes provided by PT. Cibaliung Sumberdaya. The quartz vein samples are taken from quartz vein intercept in drill core DRK05 at 54 m, DRK16 at 75 m, DRK18 at -60, DRK03 at 124, and DRK11 at 40 m above sea level, respectively. The quartz vein samples from these holes were used to characterize the quartz texture, ore mineral assemblage, and fluid inclusion microthermometry of the Rorah Kadal vein. In addition, 17 representative host rock samples from drill cores and surface outcrops were also collected for petrographic and alteration mineralogy analyses.

Polished and thin sections were observed using a transmitted and reflected light Nikon Eclipse E600 POL microscope. The ore mineral compositions were determined semi-quantitatively using a Shimadzu SEM-EDX Superscan SS550 analyzer with operational conditions that utilized a 20 kV voltage with a beam current of 10 nA, focused to 1-10 μm for 100 s.

Altered host rocks were examined using X-ray diffractometry (RIGAKU Ultima IV) with a Cu $K\alpha$ X-ray source operating under conditions of 40 kV and 20 mA with scan speed set at $2^\circ/\text{minute}$.

Doubly polished thick sections of 200 μm were prepared for fluid inclusion microthermometry. The results obtained from quartz were measured for homogenization temperature (T_h) and ice melting temperature (T_m) using a Linkam LK600 heating and cooling system. Salinity was calculated based on the equations in Bodnar (1993) [11].

Results

Lithology

The Rorah Kadal vein is hosted by volcanic breccia, lava flow deposit, and tuff of the Honje Formation. Volcanic breccia is the major host rock observed throughout all drill cores (Figure 3). From visual observation, the volcanic breccia shows an open-closed fabric, poor sorting, and compaction. The volcanic breccia is composed of rock clast, quartz, and mafic minerals and exhibits medium to intensive alteration (Figure 4a). Microscopically, the volcanic breccia is also cut by veinlets of quartz and calcite (Figure 4b), with sparsely scattered pyrite and chalcopyrite.

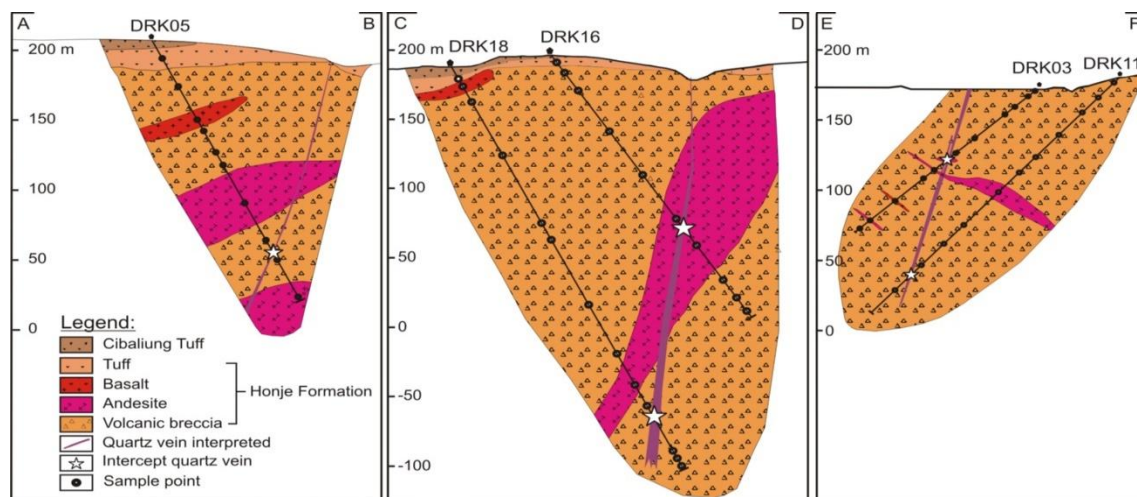


Figure 3. Simplified lithologic profile and quartz vein morphology interpretation from five drill holes

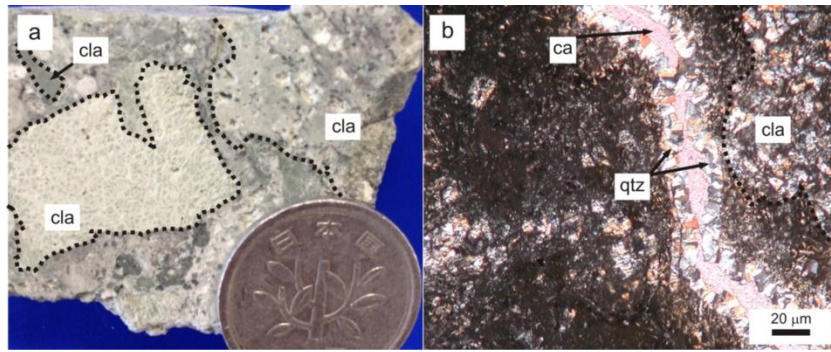


Figure 4. Photograph and photomicrograph of the argillic altered volcanic breccia. (a) The rock shows compacted and poor sorting textures. (b) A veinlet of quartz + calcite and silicified clast. Abbreviations: ca, calcite; cla, clast; qtz, quartz

The volcanic breccia is intercalated with the lava flow deposit. The lava flow deposits are characterized by basalt to andesite compositions. The andesite rocks are characterized by porphyritic textures comprising phenocrysts of plagioclase, clinopyroxene and hornblende in aphanitic groundmass (Figure 5a, b). This unit shows a weak to intermediate prophyritic alteration and is also locally cut by quartz veinlets. Basalt rocks are recognized in drill cores with limited distribution. The rock shows medium- to fine-grained crystals exhibiting porphyritic texture. Phenocrysts of plagioclase and pyroxene are dominant in all plates. Glomero-porphyritic clinopyroxenes were observed to be 0.1 to 1.0 mm in size (Figure 5c). The microcrystalline groundmass surrounds plagioclase, mafic minerals, and pyrite phenocrysts (Figure 5d).

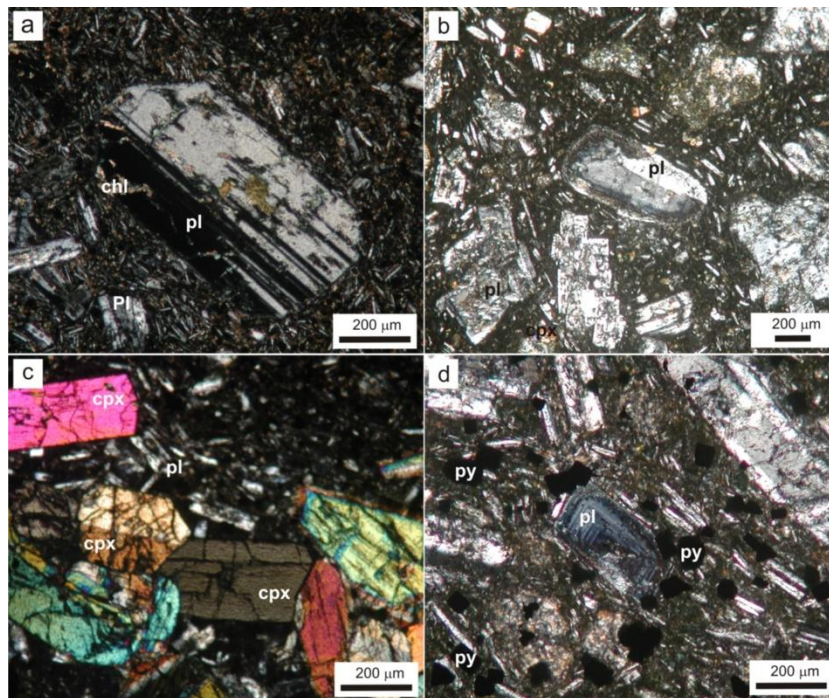


Figure 5. Photomicrographs of volcanic host rocks. a) Plagioclase phenocrysts in microcrystalline groundmass; b) Weakly altered porphyritic andesite c) Glomero-porphyritic texture of clinopyroxene in basaltic rock; and d) Plagioclase zone and pyrite dissemination in andesite. Abbreviations: pl, plagioclase; cpx, clinopyroxene; py, pyrite; chl, chlorite

The tuff overlies the volcanic breccia and is mainly observed in outcrops and upper parts of drill cores. It is fine-grained, light brown in color, and is mainly composed of plagioclase, pyroxene and volcanic glass matrix. This rock unit is strongly altered to clay minerals, locally shows reddish to yellowish color due to weathering processes and oxidized to become hematite-goethite.

Hydrothermal Alteration

Based on mineral assemblages, the alteration minerals in the Rorah Kadal vein can be grouped into three alteration zones:

Illite/smectite-adularia-quartz zone is represented in the vein zone. The vein zone is composed mainly of quartz with comb, microcrystalline, colloform-crustiform, and massive textures. There are two quartz vein phases in DRK03 that exhibit alteration: micro-crystalline quartz-illite/smectite (qtz-1) and quartz-adularia-illite/smectite (qtz-2) (Figure 6a, b). Moreover, illite/smectite mixed layer mineral is observed in hydrothermal breccia, and kaolinite was identified as vug fillings (Figure 7a), as well as iron oxide minerals like hematite.

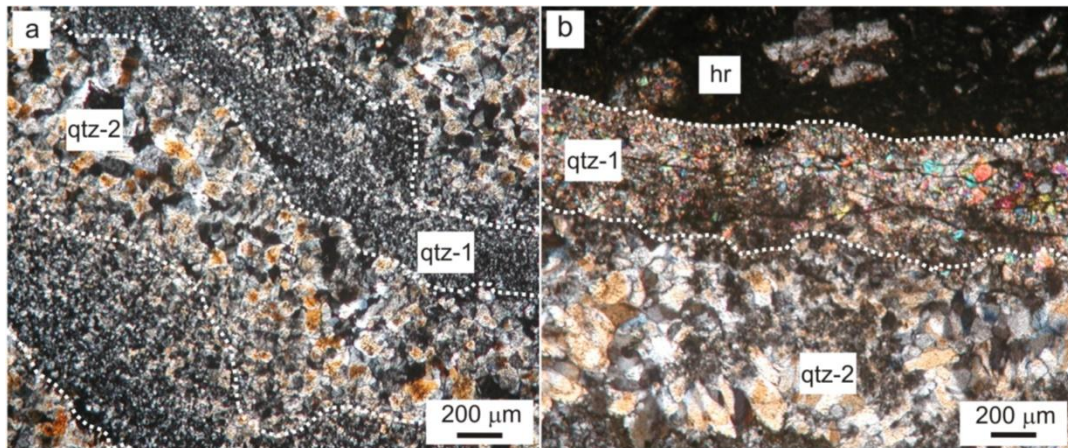


Figure 6. Photomicrographs of the hydrothermally altered rocks showing alteration variation of quartz vein and veinlets. a) Repetition of quartz textures; b) Sharp contact between host rock and quartz vein. Abbreviations: hr, host rock; qtz-1, quartz-illite/smectite; qtz-2, quartz-illite/smectite-adularia

Chlorite-chlorite/smectite mixed layer mineral zone is present within the footwall and hanging wall distal to the Rorah Kadal vein zone and confirmed by XRD analysis (Figure 7b). This type of alteration is observed in the host rock in lower parts of the drill core. In surface exposures, it is represented by the gray to greenish color of basaltic andesite host rock. Most of the primary minerals of the basalt-andesite and volcanic breccia host rocks have been replaced by chlorite, calcite and locally quartz and rare chlorite/smectite mixed layer mineral. Plagioclase phenocrysts and groundmass partially replaced by chlorite/smectite mixed layer mineral, chlorite, and quartz minerals. Secondary quartz mainly replaced the groundmass or matrix of the volcanic rocks.

Illite/smectite-calcite-quartz zone mainly occurs at the surface or near surface according to drill hole data. This alteration replaces the volcanic breccia and tuff host rocks. Most of the primary minerals are replaced by illite/smectite mixed layer mineral. Pyrite also occurs within this zone and it is rarely associated with hematite. Fine-grained secondary quartz serves as the main replacement of the tuff matrix. In addition, kaolinite is

observed coexisting with illite and filling in vugs of the vein breccias. Late-phase quartz-calcite and quartz-chlorite-pyrite veinlets also occurs as fracture filling as well (Figure 8a, b).

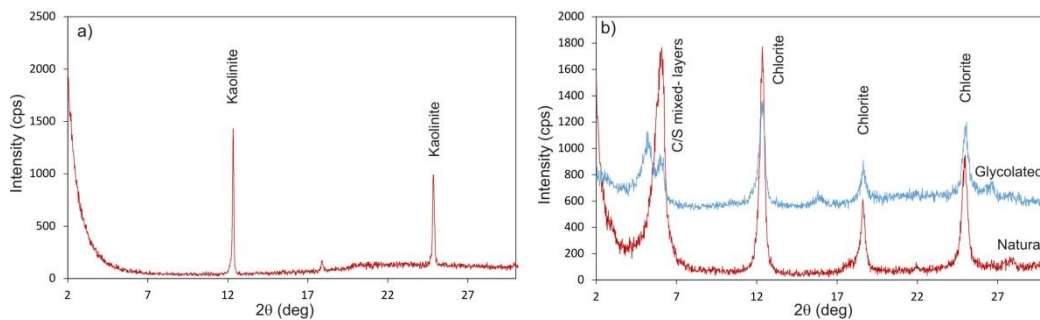


Figure 7. Representative X-ray diffraction pattern of alteration minerals. a) Kaolinite mineral. b) Chlorite+chlorite/smectite mixed-layers

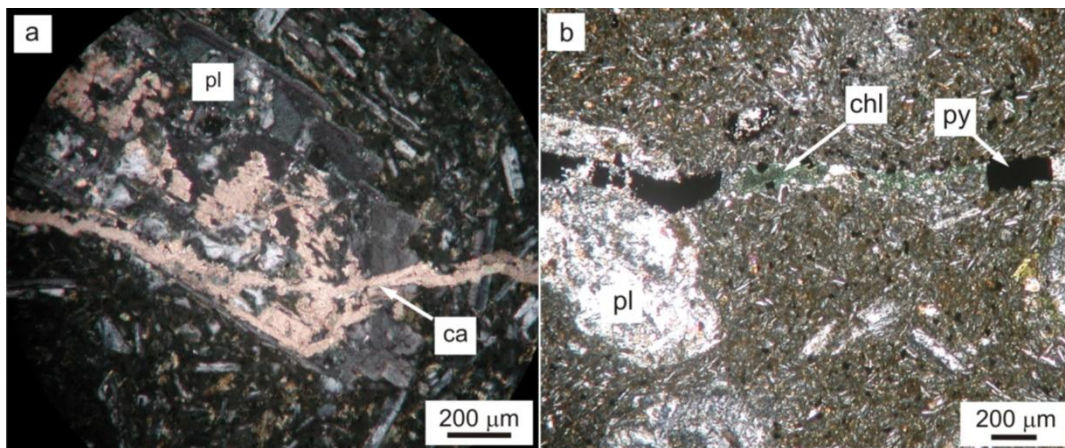


Figure 8. Photomicrograph of host rock cut by late stage veinlets. a) Calcite veinlet cutting the plagioclase phenocryst; b) Altered porphyritic andesite intruded by quartz veinlet containing chlorite and pyrite. Abbreviations: pl, plagioclase; py, pyrite; chl, chlorite; ca, calcite

Vein Characteristics

Rorah Kadal is a single vein that extends for about 250 m in strike-length and over 150 m in depth. The vein is varying in thickness, from a few centimeters at the surface up to less than 3 meters in the drill core. The quartz vein color varies from colorless, white, and pale gray to brown, with textures ranging from fine to coarse crystalline and chalcedonic.

In general, the vein is differentiated into three major textures: 1) colloform-crustiform, 2) hydrothermal breccia, and 3) late stage quartz veinlet textures. This sequence also represents the mineralization phases within the vein. Hydrothermal breccia texture is observed at drill core DRK05 (Figure 9a, b). It is composed of clasts of host rocks that are cemented by fine quartz and siliceous materials with fine-grained disseminations of pyrite. Colloform-crustiform textures are common characteristic features of quartz-chalcedonic aggregates in fine rhythmic and repetitive bands at drill core DRK03 (Figure 9c, d). This texture is characterized mainly by pale gray to whitish quartz, thin layers of dark-colored bands of sulfide minerals, and pinkish-light yellow color of adularia-illite layers and calcite in selected areas. Massive quartz is characterized by its white to milky color, and locally consists of vugs with very fine quartz crystals with rare disseminations of pyrite.

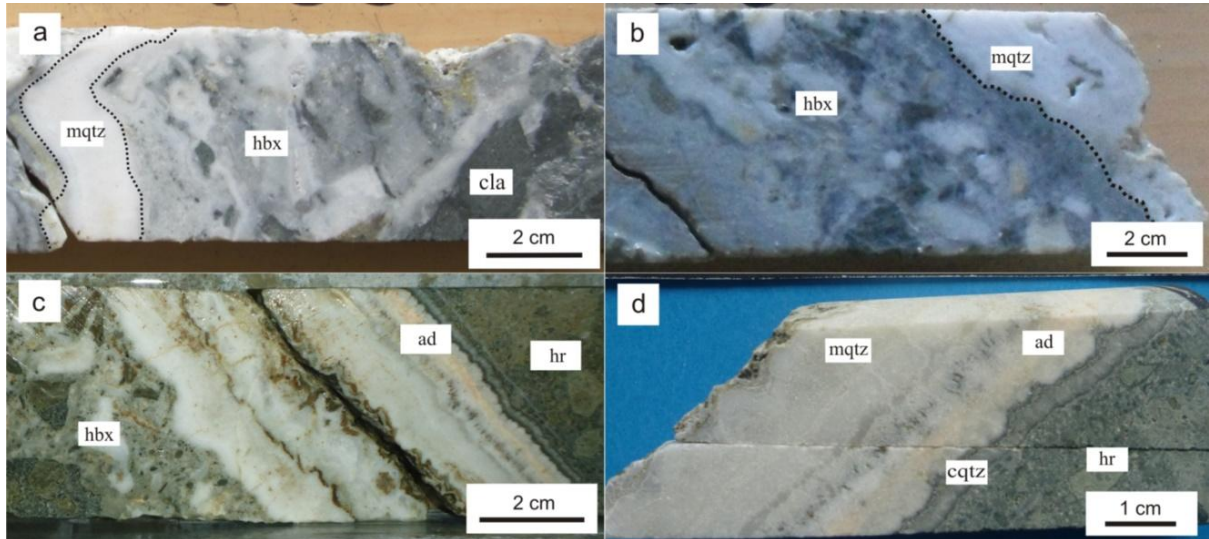


Figure 9. Sample photos of typical textures of the Rorah Kadal vein. (a) Hydrothermal breccia cut by late stage milky quartz veinlet. (b) Hydrothermal breccia in contact with vugs of milky quartz. (c) Colloform-stratiform bands in sharp contact with the host rock and hydrothermal breccia. (d) Colloform-stratiform quartz texture in contact with host rock. Abbreviations: mqtz, milky quartz; cla, clast; ad, adularia; hr, host rock; hbx, hydrothermal breccia; cqtz, comb quartz

The colloform-crustiform texture of the Rorah Kadal quartz vein and its mineralogy is observed in detail from DRK03. The vein can be classified into eleven temporal vein layers with their associated sulfide minerals as follow (Figure 10):

- a. Yellowish brown color of very fine-grained quartz, with pyrite and rare chalcopyrite
- b. Thin dark band with dominant pyrite and rare electrum
- c. Coarse- to fine-grained quartz with comb texture, mostly barren
- d. Thin, dark sulfide band with dominant pyrite, chalcopyrite, and rare electrum
- e. Medium-grained sugary quartz with dark needle-like clusters of chalcopyrite, pyrite, galena, sphalerite and electrum
- f. Very fine milky quartz with illite
- g. Banded quartz with prismatic adularia and illite/smectite mixed layer mineral
- h. Very fine milky quartz with illite
- i. Light gray band with disseminations of sphalerite, silver minerals, and electrum with sparse chalcopyrite and galena
- j. Very fine milky quartz with illite/smectite mixed layer mineral
- k. Micro-crystalline quartz, mostly massive

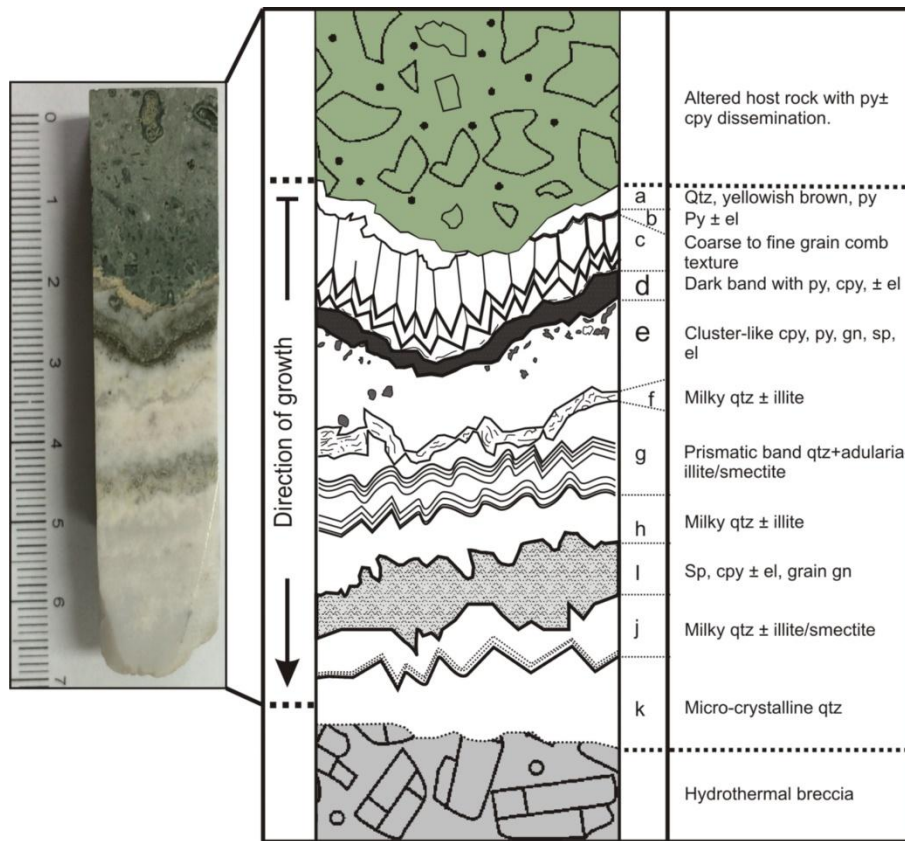


Figure 10. Simplified image of typical Rorah Kadal colloform-crustiform quartz vein (DRK03). Abbreviations: py, pyrite; el, electrum; gn, galena; sp, sphalerite; cpy, chalcopyrite; qtz, quartz

Ore and Gangue Mineralogy

The ore mineral assemblages of the Rorah Kadal vein is dominated by pyrite, chalcopyrite, galena, sphalerite, electrum, and aguilarite. Predominant gangue minerals include quartz, calcite, and adularia, with limited hematite-goethite.

Pyrite (FeS_2) is the most dominant sulfide mineral in the Rorah Kadal vein. It occurs as dissemination in host rock and in fracture filling. Pyrite is euhedral to subhedral in shape, with wide range of grain size from 10 μm to 1 mm, and coexistence with chalcopyrite. Chalcopyrite ($CuFeS_2$) occurs as grains less than 100 μm in diameter, mostly as a single crystal and coexisting with chalcopyrite, aguilarite and rare with electrum (Figure 11a).

Galena (PbS) is observed as single crystal and sometimes coexisting with other sulfide minerals such as chalcopyrite, sphalerite, and aguilarite (Figure 11b). The grains are about 5 to 15 μm in diameter. Sphalerite (ZnS) occurs as single crystals, fine to medium up to 50 μm in diameter.

The electrum ($AuAg$) is found in colloform-crustiform stages in the quartz vein. Electrum is associated with chalcopyrite and aguilarite (Figure 11c), and also occurs as single grains (Figure 9d). They are anhedral in shape, and less than 15 μm in size. SEM-EDX analysis revealed that the composition of gold in electrum ranges between 46.2-69.4 wt % and the silver is 30.6-53.8 wt%.

Silver minerals also occurs as fine-grained crystals of aguilarite (Ag_4SeS). This mineral exist with chalcopyrite, galena, and sphalerite (11d). Aguilarite size up to 25 μm . These minerals are found as part of a stage in colloform-crustiform quartz band.

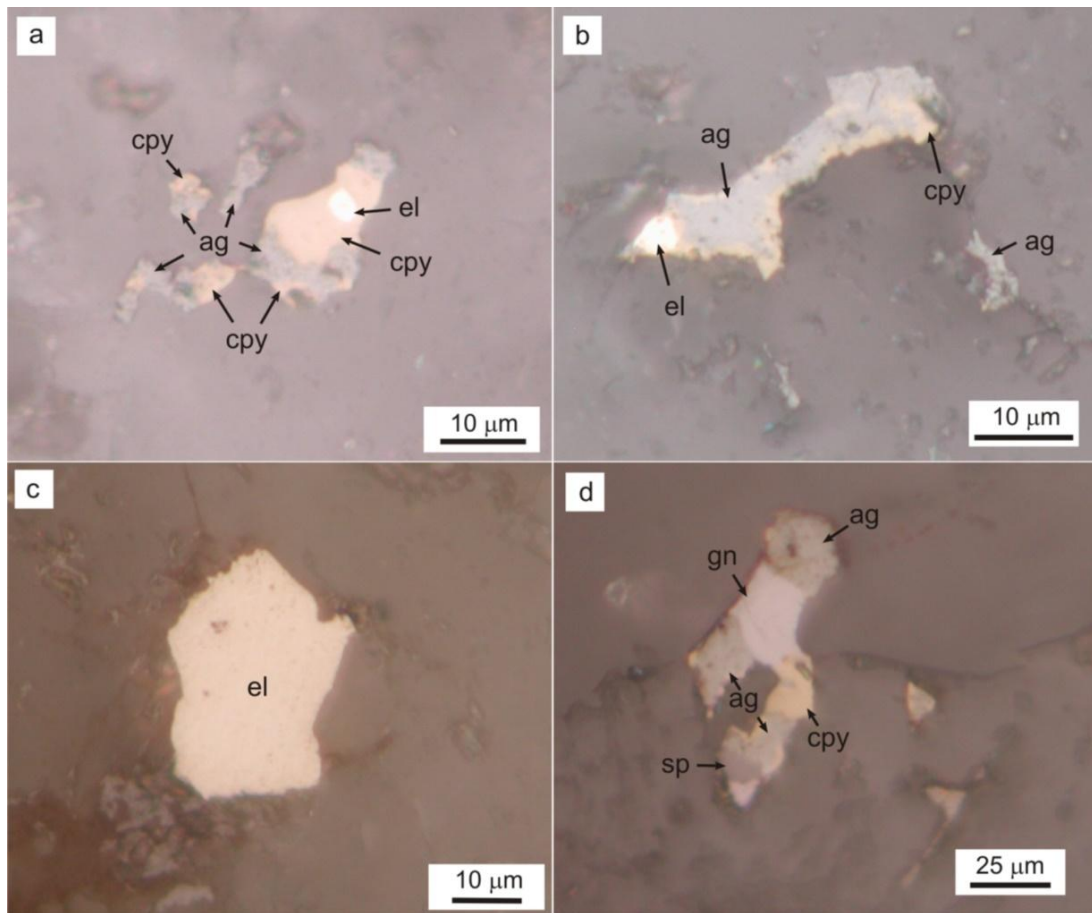


Figure 11. Photomicrographs of ore minerals in Rorah Kadal quartz vein. (a, b) Electrum coexisting with chalcopyrite and aguilarite, (c) A single electrum crystal, (d) Aguilarite coexisting with sphalerite, galena, and chalcopyrite. Abbreviations: el, electrum; cpy, chalcopyrite; ag, aguilarite; gn, galena; and sp, sphalerite

Fluid Inclusion Microthermometry

The fluid inclusion microthermometry measurement was conducted on quartz samples from drill cores DRK03, DRK05, DRK11, and DRK16 that representing colloform-crustiform quartz bands texture and DRK18 which representing comb quartz texture (Figure 10). The vertical depth variation of the quartz vein samples are DRK03 (124 m); DRK16 (75 m); DRK05 (54 m); DRK11 (40 m); and DRK18 (-60 m) (Figure 3). Primary inclusions are used for temperature homogenization and salinity [10]. The criteria to determine the primary liquid-vapor inclusions and evidence of boiling are derived from [11,12]. Temperatures of homogenization (T_h) and temperatures of final melting point of ice (T_m) were measured for representative inclusions.

The inclusions are small in size, elongated to sub-rounded in shape, and solitary (Figure 12a, b, c). The size of fluid inclusions range from 5 to 25 μm . Two types of fluid inclusions are visible at room temperature: two-phase liquid rich and two-phase liquid-vapor rich inclusions. The majority of inclusions are generally classified as liquid-rich with a liquid and vapor ratio of approximately 5:1. Sub-dendritic growth in mechanism of trapping was observed in DRK05 quartz sample (12d).

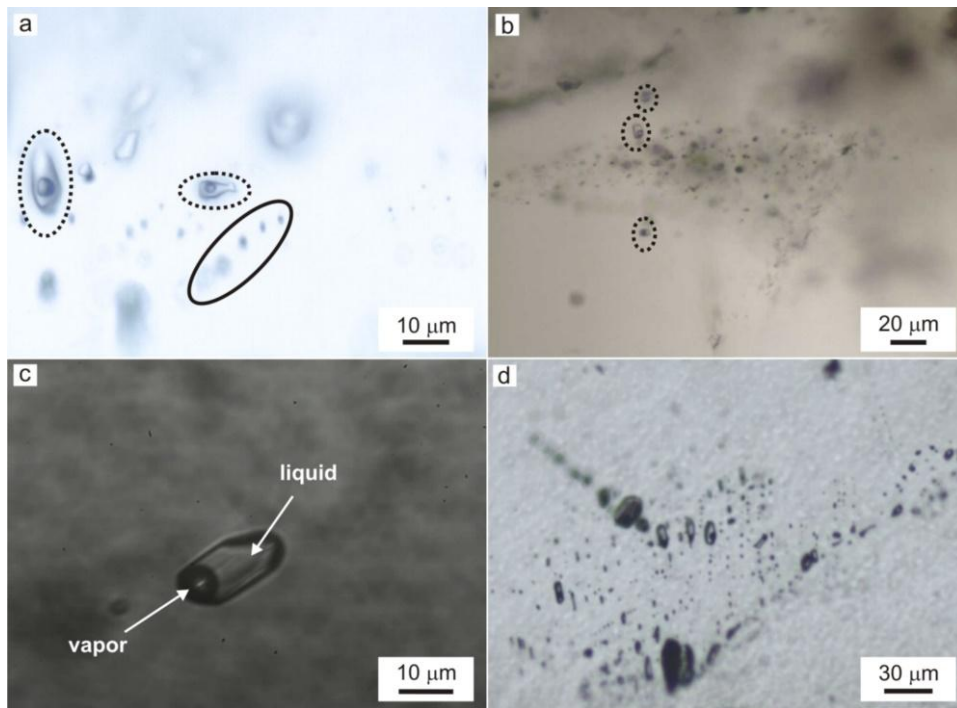


Figure 12. Photomicrographs of fluid inclusion shows occurrence variations in Rorah Kadal quartz vein. (a, b) Primary and secondary fluid inclusions, (c) Typical of liquid rich inclusion, (d) Sub-dendritic growth. Dashed line is primary inclusion

The results indicate that the fluid inclusions from the Rorah Kadal quartz vein have a wide homogenization temperature range (Fig. 13). The homogenization temperature (T_h) of fluid inclusions in quartz from DRK05 ranges from 200 to 330 °C, with final ice melting temperatures (T_m) of -1.5 to -0.9 °C, corresponding to salinity of 1.6 to 2.5 wt% NaCl eq. The T_h obtained from DRK16 ranges from 180 to 290 °C. The T_m was relatively low at -2.4 to -0.9 °C, corresponding to salinity of 1.6 to 4.0 wt% NaCl eq. Sample DRK18 shows a T_h range of 200-270 °C, with T_m from -1.3 to -0.8 °C, that corresponds to salinity of 1.4 to 2.2 wt% NaCl eq. The T_h measurement in quartz from DRK03 ranges from 190 to 260 °C, with melting temperatures varying from -1.8 to -0.7 °C, corresponding to a salinity range of 1.2 to 3.1 wt% NaCl eq. However, The DRK11 sample exhibits a T_h range of 190 to 310 °C. Its T_m is from -1.2 to -0.8 °C, which corresponds to a salinity range of 1.4 to 2.0 wt% NaCl eq (Table 1).

The colloform-stratiform quartz vein from DRK03 and DRK11 which exhibits the boiling phenomena, has a main mineralization temperature estimated at 190-310 °C.

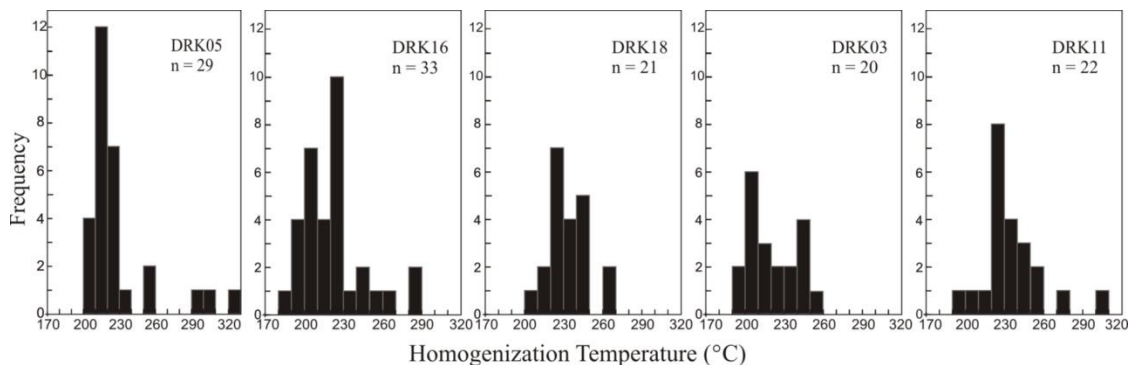


Figure 13. Homogenization temperature of fluid inclusions from five drill cores indicated that all the quartz samples have a wide range from 180 to 330 °C

Table 1. Microthermometry Data from Quartz Fluid Inclusions in the Rorah Kadal Vein

| Sample Name | Size (μm) | T_h Range ($^{\circ}\text{C}$) | T_h Mode ($^{\circ}\text{C}$) | T_m Range ($^{\circ}\text{C}$) | Salinity Range (wt% NaCl eq.) |
|-------------|------------------------|------------------------------------|-----------------------------------|------------------------------------|-------------------------------|
| DRK05 | 6-33 | 200-330 | 210 | -1.5 to -0.9 | 1.6-2.5 |
| DRK16 | 4-20 | 180-290 | 220 | -2.4 to -0.9 | 1.6-4.0 |
| DRK18 | 8-20 | 200-270 | 220 | -1.3 to -0.8 | 1.4-2.2 |
| DRK03 | 6-30 | 190-260 | 200 | -1.8 to -0.7 | 1.2-3.1 |
| DRK11 | 7-35 | 190-310 | 220 | -1.2 to -0.8 | 1.4-2.0 |

Discussion

The gold prospect in the Rorah Kadal quartz vein is hosted by the Honje Formation, which consist of breccia volcanic intercalated with lava flow deposits with composition of basaltic to andesitic rock intercalated with breccia volcanic and overlay by tuff. The age of host rock is 11.4 Ma while the age of mineralization is 11.18-10.65 Ma [4].

There are three alteration zones in this prospect, illite/smectite-adularia-quartz, chlorite-chlorite/smectite mixed layer minerals, and illite/smectite-calcite-quartz zone. The alteration assemblages indicate formation by near-neutral fluids in the hydrothermal system [14]. The Illite/smectite-adularia-quartz alteration zone is an important phase for ore mineralization in this prospect. The gold-silver mineralization is associated with the quartz-illite/smectite and quartz-adularia illite/smectite. The occurrence of adularia within the colloform-crustiform quartz vein texture also indicates the possibility of boiling; Banding in the vein represents the occurrence of continuous cooling as a result of fluid mixing with the lower temperature meteoric water, which could be a possible ore depositional mechanism[14-15].

The hydrothermal stages of Rorah Kadal can be ordered as follows: 1- colloform-crustiform banded quartz, 2- hydrothermal breccia, and 3- comb-massive quartz. Here, the main ore mineralization takes place during the colloform-crustiform banding stage. Gold occurs mainly as electrum and coexists with chalcopyrite in the colloform-crustiform banding.

The ore mineral assemblage in the Rorah Kadal quartz vein is composed of dominant pyrite with various amounts of chalcopyrite, galena, sphalerite, electrum, and aguilarite. This composition is similar to the Gunung Pongkor vein system [19-20], and Cikidang vein [2] located in the Bayah Dome Complex which are typical low sulfidation epithermal deposits. The ore mineralogy is similar to the Cibitung and Cikoneng veins included within the Cibaliung goldfield [3, 5, and 16]. However in Rorah Kadal quartz vein, primary gold is present as electrum and in single-grains, and mostly associated within the colloform-crustiform banded quartz.

Fluid inclusion microthermometry data from quartz shows T_h range from 180-330 $^{\circ}\text{C}$ both in colloform-crustiform quartz and comb texture with the salinity varying between 1.2 to 4.0 wt% NaCl eq. The results indicated that all quartz samples representing the same stage of mineralization. The low salinity and range T_h from < 100 to 330 $^{\circ}\text{C}$ are typical for epithermal deposits. In addition, liquid-rich inclusions are also typical for low-sulfidation epithermal deposits[18,19]. The trapping temperature of the boiling zone is calculated from the first peak in the histogram of homogenization temperature [5, 13], and 21]. Plotting the mode of homogenization temperature on the boiling point curve [22], the depth of mineralization from the paleo water table level was revealed to be at 169 - 259 meters and pressure is estimated to be around 18-27 bars (Fig.14). Erosion is estimated range from 45

to 319 meters. This suggests of absence of silica sinter as a paleosurface indicator in this hydrothermal system.

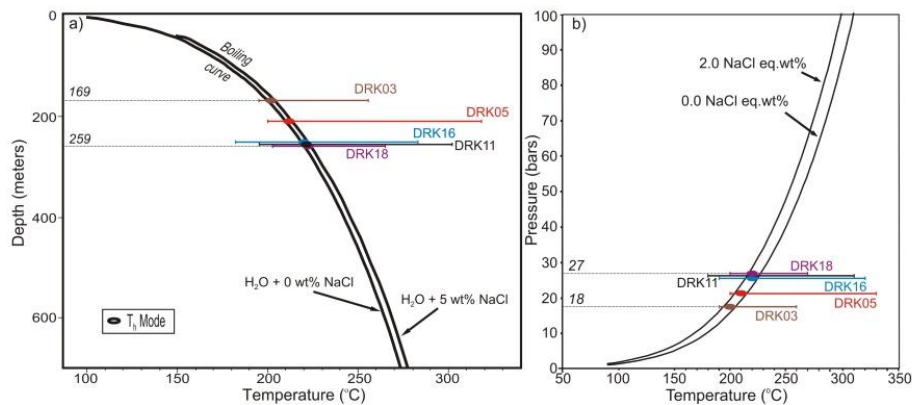


Figure 14. a) Estimated mineralization depth is at 169-259 m based on the mode of boiling curve diagram of ; b) From the homogenization temperature measurements, the inferred pressure is estimated at 18-27 bars [22]

Based on fluid inclusion microthermometry study, the Rorah Kadal quartz vein has slightly high fluid temperature and salinity as compared to Cikoneng and Cibitung veins of the Cibaliung goldfield. The Rorah Kadal vein has temperature T_h range from 180-330 °C with the salinity between 1.2 to 4.0 wt% NaCl eq. Meanwhile, the Cikoneng has temperature T_h range from 210-270 °C with the salinity between 0.1 to 0.6 wt% NaCl eq., and the Cibitung has temperature T_h range from 200-250 °C with the salinity between 0.5 to 1.1 wt% NaCl eq.[23]. However, it is difficult to interpret that Cikoneng, Cibitung and Rorah Kadal veins are resulted from similar fluid and similar vein system. It will be need more study to prove.

Conclusions

The alteration can be classified into three zones, namely illite/smectite-adularia-quartz, chlorite-chlorite/smectite mixed layer mineral, and illite/smectite-calcite-quartz zones respectively. The mineralization stages of the Rorah Kadal quartz vein can be classified into: colloform-crustiform banded, hydrothermal breccia, and late stage quartz veinlet textures. The ore mineralogy is composed of dominant pyrite with various amounts of chalcopyrite, galena, sphalerite, electrum, and aguilarite. Fluid inclusions data from quartz samples show T_h range from 182-302 °C with the salinity varying between 1.2 to 4.0 wt% NaCl eq. The calculated mineralization depth are 249-333 m below the paleo water table. The Rorah Kadal vein has slightly high fluid temperature and salinity as compared to Cikoneng and Cibitung veins of the Cibaliung goldfield.

Based on the study of alteration, ore mineralogy, and fluid inclusion microthermometry the Rorah Kadal quartz vein appears to have formed from low temperature and low salinity fluids in near-neutral pH environment.

Acknowledgments

First author acknowledges to DGHE of the Indonesia Government for granting Ph.D. scholarship and G-COE Program of Kyushu University for financial support. The authors

are very grateful to PT. Cibaliung Sumberdaya and PT Antam Tbk for permission to use and publish the data.

References

- [1] E. Marcoux, and J.P. Milési, "Epithermal gold deposits in West Java, Indonesia: Geology, age and crustal source," *Journal of Geochemical Exploration*, Vol. 50, No. 1-3, pp. 393-408, 1994.
- [2] M.F. Rosana, and H. Matsueda, "Cikidang hydrothermal gold deposit in Western Java, Indonesia," *Resource Geology*, Vol. 52, No. 4, pp. 341-352, 2002.
- [3] C.A. Angeles, S. Prihatmoko, and J.S. Walker, "Geology and alteration-mineralization characteristics of the Cibaliung epithermal gold deposit, Banten, Indonesia," *Resource Geology*, Vol. 52, No. 4, pp. 329-339, 2002.
- [4] A. Harijoko, K. Sanematsu, R.A. Duncan, S. Prihatmoko, and K. Watanabe, "Timing of the mineralization and volcanism at Cibaliung gold deposit, Western Java, Indonesia," *Resource Geology*, Vol. 54, No. 2, pp. 187-195, 2004.
- [5] A. Harijoko, Y. Ohbuchi, Y. Motomura, A. Imai, and K. Watanabe, "Characteristics of the Cibaliung gold deposit: Miocene low-sulfidation-type epithermal gold deposit in Western Java, Indonesia," *Resource Geology*, Vol. 57, No. 2, pp. 114-123, 2007.
- [6] S. Prihatmoko, B. Trisetyo, D. Moku, D. Kusumanto, and D. Setyono, *Geology Progress Report*, Unpublished report, p. 94, 2004.
- [7] J.C. Carlile, and A.H.G. Mitchell, "Magmatic arcs and associated gold and copper mineralization in Indonesia," *Journal of Geochemical Exploration*, Vol. 50, No. 1-3, pp. 91-142, 1994.
- [8] J.P. Miliés, E. Marcoux, T. Sitorus, M. Simandjuntak, J. Leroy, and L. Bailly, "Pongkor (west Java, Indonesia): A Pliocene supergene-enriched epithermal Au-Ag-(Mn) deposit," *Mineralium Deposita*, Vol. 34, No. 2, pp. 131-149, 1999.
- [9] R. Marjoribanks, *Geology of the Honje-Cibaliung Area, West Java, Indonesia - An Air Photo Interpretation Based Study*, Unpublished Report, p. 13, 2000.
- [10] D. Sudana, and S. Santosa, *Geology of the Cikarang Quadrangle, Java*, Geology Research Development Center, Bandung, p. 13, 1992.
- [11] R.J. Bodnar, "Revised equation and table for determining the freezing point depression of H₂O-NaCl solutions," *Geochimica et Cosmochimica Acta*, Vol. 57, No. 3, pp. 683-684, 1993.
- [12] E. Roedder, *Fluid Inclusions: An Introduction to Studies of All Types of Fluid Inclusions, Gas, Liquid, Or Melt, Trapped in Materials from Earth and Space, and Their Application to the Understanding of Geologic Processes*, Review in Mineralogy Vol. 12, Mineralogical Society of America, United States, 1984.
- [13] R.J. Bodnar, T.J. Reynolds, and C.A. Kuehn, "Fluid-inclusion systematics in epithermal systems," In *Geology and Geochemistry of Epithermal Systems (Reviews in Economic Geology Vol. 2)*, B.R. Berger, and P.M. Bethke, eds.: Society of Economic Geologists, El Paso, Texas, United States, pp. 73-97, 1985.
- [14] J.W. Hedenquist, E. Izawa, A. Arribas, and N.C. White, *Epithermal Gold Deposits: Styles, Characteristics, and Exploration*, Resource Geology Special Publication No. 1, Society of Resource Geology of Japan, 1996.
- [15] D. Moncada, S. Mutchler, A. Nieto, T.J. Reynolds, J.D. Rimstidt, and R.J. Bodnar, "Mineral textures and fluid inclusion petrography of the epithermal Ag-Au deposits at Guanajuato, Mexico: Application to exploration," *Journal of Geochemical Exploration*, Vol. 114, pp. 20-35, 2012.
- [16] J.W. Hedenquist, E. Izawa, A.J. Arribas, and N.C. White, *Epithermal Gold Deposits: Styles, Characteristics, and Exploration*, Resource Geology Special Publication No. 1, Society of Resource Geology of Japan, 1996.

- [17] A. Basuki, D.A. Sumanagara, and D. Sinambela, "The Gunung Pongkor gold-silver deposit, West Java, Indonesia," *Journal of Geochemical Exploration*, Vol. 50, No. 1-3, pp. 371-391, 1994.
- [18] I.W. Warmada, B. Lehmann, W. And, and M. Simandjuntak, "Polymetallic sulfides and sulfosalts of the Pongkor epithermal gold-silver deposit, West Java, Indonesia," *The Canadian Mineralogist*, Vol. 41, No. 1, pp. 185-200, 2003.
- [19] P. Heald, N.K. Foley, and D.O. Hayba, "Comparative anatomy of volcanic-hosted epithermal deposits: Acid-sulfate and adularia-sericite types," *Economic Geology*, Vol. 82, No. 1, pp. 1-26, 1987.
- [20] N.C. White, and J.W. Hedenquist, "Epithermal gold deposits: Styles, characteristics and exploration," *Society of Economic Geologists (SEG) Newsletter*, No. 23, pp. 1, 9-13, 1995.
- [21] J. Etoh, E. Izawa, and S. Taguchi, "A fluid inclusion study on columnar adularia from the Hishikari low-sulfidation epithermal Gold Deposit, Japan," *Resource Geology*, Vol. 52, No. 1, pp. 73-78, 2002.
- [22] J.L. Haas, Jr., "The effect of salinity on the maximum thermal gradient of a hydrothermal system at hydrostatic pressure," *Economic Geology*, Vol. 66, pp. 940-946, 1971.
- [23] M.F. Rosana, S. Prihatmoko, and T. Setiabudi, "Low-sulfidation epithermal Au mineralization in Western Java and Southern Sumatra: Characteristics and their exploration implication," In *Sundaland Resources*, Palembang, Indonesia, pp. 109-128, 2014.